Macromolecular Research

Volume 13, Number 3 June 30, 2005

Review

Self-Assembled Nanoparticles of Bile Acid-Modified Glycol Chitosans and Their Applications for Cancer Therapy

Kwangmeyung Kim,[1,2] Jong-Ho Kim,[1,2] , Sungwon Kim,[1] Hesson Chung,[1] Kuiwon Choi,[1] and Ick Chan Kwon[1,2]*

[1]*Biomedical Research Center, Korea Institute of Science and Technology, Seoul 136-791, Korea*
[2]*KIST Regional Laboratory in Advanced Medical Technology Cluster for Diagnosis & Prediction, Daegu 700-422, Korea*

Jae Hyung Park

Department of Advanced Polymer and Fiber Materials, College of Environment and Applied Chemistry, Kyung Hee University, Gyeonggi-do 449-701, Korea

Yoo-Shin Kim,[3,4] Rang-Won Park,[3,4] and In-San Kim[3,4]

[3]*Department of Biochemistry, School of Medicine, Kyungpook National University, Daegu 700-422, Korea*
[4]*Advanced Medical Technology Cluster for Diagnosis & Prediction, Daegu 700-422, Korea*

Seo Young Jeong

Department of Pharmaceutics, College of Pharmacy, Kyung Hee University, Seoul 130-701, Korea

Received March 21, 2005; Revised April 1, 2005

Abstract: This review explores recent works involving the use of the self-assembled nanoparticles of bile acid-modified glycol chitosans (BGCs) as a new drug carrier for cancer therapy. BGC nanoparticles were produced by chemically grafting different bile acids through the use of 1-ethyl-3-(3-dimethylaminopropyl)-carbodiimide (EDC). The precise control of the size, structure, and hydrophobicity of the various BGC nanoparticles could be achieved by grafting different amounts of bile acids. The BGC nanoparticles so produced formed nanoparticles ranging in size from 210 to 850 nm in phosphate-buffered saline (PBS, pH=7.4), which exhibited substantially lower critical aggregation concentrations (0.038-0.260 mg/mL) than those of other low-molecular-weight surfactants, indicating that they possess high thermodynamic stability. The BGC nanoparticles could encapsulate small molecular peptides and hydrophobic anticancer drugs with a high loading efficiency and release them in a sustained manner. This review also highlights the biodistribution of the BGC nanoparticles, in order to demonstrate their accumulation in the tumor tissue, by utilizing the enhanced permeability and retention (EPR) effect. The different approaches used to optimize the delivery of drugs to treat cancer are also described in the last section.

Keywords: glycol chitosan, nanoparticle, EPR effect, cancer therapy.

*e-mail: ikwon@kist.re.kr
1598-5032/06/167-09©2005 Polymer Society of Korea

Introduction

Polymeric amphiphiles consisting of hydrophilic and hydrophobic segments have attracted a great deal of attention as drug carriers, because they can form self-assembled nanoparticles and exhibit unique physicochemical characteristics in aqueous media.[1-5] Various polymeric amphiphiles undergo intra- or intermolecular association, promoted primarily by interactions between the hydrophobic segments. Such interactions allow the polymers to form micelles or nanoparticles, possibly having unusual rheological features, a small hydrodynamic radius with a core-shell structure, and thermodynamic stability. In aqueous media, their hydrophobic cores are surrounded by hydrophilic outer shells, so that the inner core can serve as a nano-container for various peptides and drugs.

Polymeric nanoparticles exhibit a prolonged circulation time in the blood stream by avoiding the reticuloendothelial system (RES), and this reduced liver and spleen uptake has been exploited in the treatment of solid tumors, because the prolonged circulation time of the nanoparticles allows them to accumulate and extravasate into the tumor tissue, in which a disorganized vasculature and defective vascular architecture develop. This attribute of the tumor tissue, which is called an enhanced permeation and retention (EPR) effect,[8] enables macromolecules or nanoparticles to accumulate in it. Therefore, the use of polymeric nanoparticles has been recognized as an effective strategy for passive tumor targeting.[9-13]

Chitosan, which is primarily composed of 2-amino-deoxy-β-*D*-glucopyranose (*D*-glucosamine), is the deacetylated derivative of chitin, which is the second most abundant natural polysaccharide.[14] Owing to its biocompatibility, biodegradability and low immunogenicity, interest in using chitosan and its derivatives in drug delivery has increased in recent years.[15,16] In particular, hydrophobically modified chitosans with hydrophobic fatty acids, bile acids, and anticancer drugs formed nano-sized self-aggregates and they showed a promising potential in drug delivery.[17-21] It has been known that hydrophobically modified chitosan nanoparticles can imbibe hydrophobic anticancer drugs with a high loading efficiency and release them in a sustained manner. However, most of the chitosan-based nanoparticles that have been developed so far had limited applicability as a drug carrier, because chitosan nanoparticles are insoluble in physiological conditions (pH=7.4) and, consequently, they are readily precipitated within a few days.[22]

Recently, water-soluble chitosan derivatives have been used to prepare polymeric nanoparticles, since they are stable in physiological conditions and, therefore, do not precipitate for a long period of time. Of these chitosan derivatives, glycol chitosan is emerging as a novel drug carrier, because of its solubility and biocompatibility in physiological conditions.[23-25] In this regard, glycol chitosan has been extensively modified with bile acids to form self-assembled nanoparticles in aqueous media.[26-29] This review deals with the application of bile acid-modified glycol chitosan (BGC) nanoparticles to cancer therapy. The structure of BGC nanoparticles is stable in physiological conditions and, consequently, they have the potential to be used as drug carriers for anticancer peptides and drugs. Finally, the *in vitro* and *in vivo* approaches to cancer therapy using BCG nanoparticles are described.

Synthesis of Bile Acid-Modified Glycol Chitosan (BGC) Derivatives

The chemical modification of glycol chitosan, the 6-(2-hydroxyethyl) ether derivative of chitosan, provides a powerful method of endowing it with new biological activities and of modifying its physicochemical properties. The primary amine groups of glycol chitosan are reactive and provide diverse possibilities for side group attachment using various chemical graft reactions with fatty acids, bile acids, and drugs.[17,19,26,29] Thus, a variety of groups can be grafted to glycol chitosan, which can be selectively chosen to provide specific functionality and various biological properties.

To produce amphiphilic glycol chitosan derivatives, bile acids (deoxycholic acid or 5-β-cholanic acid) were introduced into the glycol chitosan backbone, because they are known to form micelles in water due to their amphiphilicity, which play an important role in the emulsification, solubilization and absorption of cholesterol, fats, and lipophilic vitamins in the body.[30] Thus, it was expected that the introduction of bile acids into the glycol chitosan molecule would induce its self-association to form a nanoparticle structure in aqueous media.

BGC derivatives (DGC; deoxycholic acid-modified glycol chitosan, CGC; 5-β-cholanic acid-modified glycol chitosan) were simply prepared by the esterification of the carboxylic group in deoxycholic acid or cholanic acid and the amine groups in glycol chitosan using 1-ethyl-3-(3-dimethylaminopropyl)-carbodiimide (EDC) and *N*-hydroxysuccinimide (NHS), because EDC reacts with the carboxyl group of deoxycholic acid or cholanic acid to form a highly reactive ester intermediate.[17,29] This intermediate can then react with the primary amine groups of glycol chitosan to form an amide bond. Based on EDC chemistry, the hydrophobicity of the glycol chitosan derivatives was simply controlled by changing the feed ratio of the bile acids (Figure 1). The degree of substitution (DS), which is defined as the number of bile acids per 100 anhydroglucosamine units of glycol chitosan, increases with increasing mole ratio of the bile acid. The DS of BGC was in the range of 1-29. Owing to the limited solubility of bile acids in aqueous media, the BGC derivatives with higher DS precipitated and did not form a nanoparticle structure. The produced BGC derivatives are summarized in Table I.

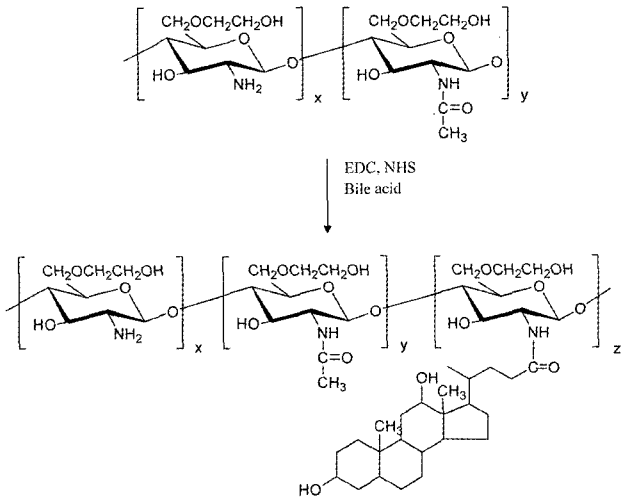

Figure 1. Chemical grafting reaction scheme between glycol chitosan and bile acid.

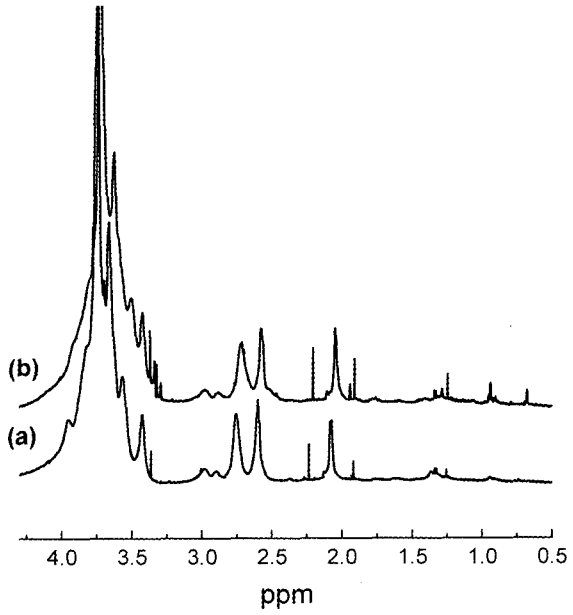

Figure 2. ^{1}H-NMR spectra of DGC30 in (a) D_2O and (b) D_2O/CD_3OD (3v/1v) (adapted from Ref. [29]).

Table I. General Properties of Self-Aggregates in PBS Solution (pH=7.4)

Sample[a]	M_n[b]	DS	x[c]	d (nm)[d]	μ_2/Γ
GC	250,000				
DGC 6	265,000	5.5	0.060	450	0.043
DGC 11	282,500	11.2	0.130	410	0.015
DGC 22	312,500	21.5	0.250	330	0.020
DGC 30	337,500	29.7	0.350	245	0.005
CGC1	255,000	1.1	0.019	850	0.043
CGC5	272,000	5.2	0.082	302	0.015
CGC12	299,000	11.5	0.165	210	0.005

[a]Glycol chitosan bearing deoxycholic acid (DGC) and 5-β-cholanic acid (CGC), in which the number indicates the DS of deoxycholic acid and 5-β-cholanic acid, respectively. [b]Number-average molecular weight, estimated from the colloidal titration results. [c]Weight fraction of deoxycholic acid and 5-β-cholanic acid. [d]Mean diameter in PBS (pH=7.4) measured by dynamic light scattering.

Physicochemical Properties of BGC Nanoparticles

Self-Aggregation of BGC Derivatives in Aqueous Media. Self-aggregates of BGC derivatives were simply produced in an aqueous media. Since amphiphilic BGC derivatives undergo intramolecular or intermolecular association in an aqueous media, promoted by hydrophobic bile acid molecules. In the ^{1}H NMR study (Figure 2), all the characteristic peaks of the glycol chitosan and deoxycholic acid groups of the DGC derivatives were clearly observed in $D_2O/CDCl_3$, whereas the peaks of the deoxycholic acids at 0.6-2.5 ppm in the ^{1}H NMR spectra were significantly decreased in D_2O. This result indicates that the molecular motion of the hydrophobic deoxycholic acid units in the hydrophobic cores is limited, because of the formation of self-aggregates in D_2O, thereby causing proton signal shielding or peak broadening of the deoxycholic acid units. This trend in the ^{1}H NMR spectra is very consistent with other polymeric amphiphiles that form micelles or nanoparticles in aqueous media.

The mean sizes of the self-aggregates (1 mg/mL in PBS buffer) were in the range of 210-850 nm, depending on the DS value of the bile acid being used, as shown in Table I. In general, the mean size of the BGC nanoparticles decreased as the DS value of the bile acid increased, and they showed a narrow size distribution. The variation in the hydrophobicity of the bile acids also affected the size of the self-aggregates. It was found that the CGC derivatives with the more hydrophobic 5-β-cholanic acid formed nanoparticles with a lower DS value, as compared to the DGC derivatives. Overall, the mean sizes of the BGC nanoparticles were larger than those based on the bile acid-modified chitosan self-aggregates (161-180 nm). The difference in solubility between chitosan and glycol chitosan would be expected to affect the size of the self-aggregates, because chitosan is not soluble, but swollen, in aqueous media at neutral pH, whereas glycol chitosan is highly soluble. The mean size of the BGC nanoparticles was scarcely affected by the concentration of the BGC nanoparticles in the range of 0.1-5 mg/mL, because the interparticle interaction between the nanoparticles is almost negligible. TEM observation demonstrated that the shape of the BGC nanoparticles is nearly spherical, as shown in Figure 3. The hydrophobically modified BGC nanoparticles were well dispersed in aqueous media and they formed a homogenous nanoparticle structure.

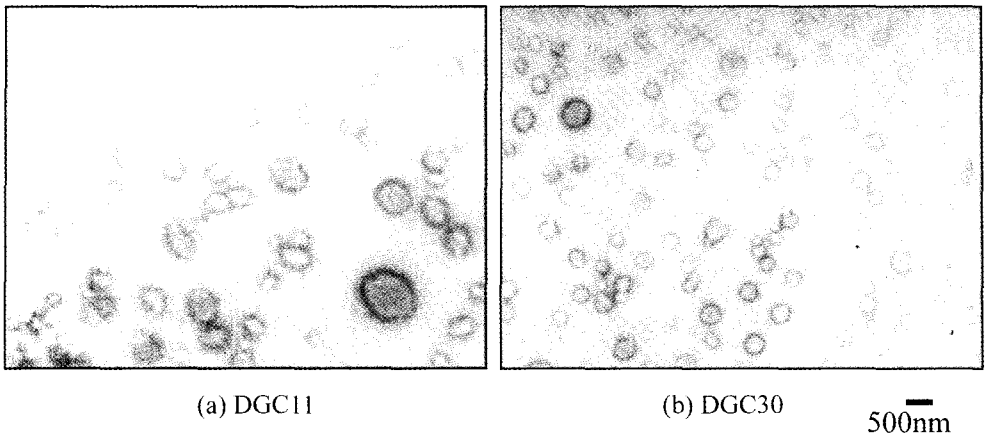

Figure 3. TEM images of DGC nanoparticles in PBS (1 mg/mL) (adapted from Ref. [29]).

The Microscopic Characteristics of BGC Nanoparticles in an Aqueous Media. The microscopic characteristics of BGC derivatives in aqueous media were investigated using a fluorometer in the presence of pyrene as a fluorescent probe.[31,32] Since pyrene molecules are preferably locate inside or close to the hydrophobic microdomains of nanoparticles rather than aqueous phase, resulting in different photophysical characteristics. The excitation spectra of pyrene in DGC30 solution was obtained as a function of the DGC30 concentration. As shown in Figure 4, the excitation spectra shows peaks for the (0.0) band at 338 nm in the low concentration range, indicating that DGC30 does not form aggregates in dilute solution. As the concentration increased, the peaks were shifted to 343 nm and the intensity increased markedly. This result indicates that chemically grafted deoxycholic acids start to form hydrophobic cores in an aqueous media, which was defined as a critical aggregation concentration (cac). The cac could be determined from the graph of the intensity ratio (I_{343}/I_{338}) of the pyrene excitation spectra versus the logarithm of the BGC derivatives concentration. The cac values of the BGC derivatives decreased as the content of hydrophobic deoxycholic acid or cholanic acid increased, because of the resulting enhanced hydrophobicity, as shown in Table I. The cac values of the BGC derivatives were in the range of 0.038-0.260 mg/mL, which is lower than those of low molecular weight surfactants (e.g., 1.0 mg/mL for deoxycholic acid and 2.3 mg/mL for sodium dodecyl sulfate in water), but were larger than those of other di-block polymeric amphiphiles (0.013-0.045 mg/mL). It may be that the stiff glycol chitosan backbone hampered the formation of the dense hydrophobic cores composed of bile acid molecules.[21]

The hydrophobicities of the inner cores of the BGC nanoparticles, based on the equilibrium constants (K_v) for the partitioning of pyrene between the water and nanoparticle phase shown in Table II, were in the range of 0.4 - 4.0 $\times 10^4$. The hydrophobicities of the inner cores of the nanoparticles

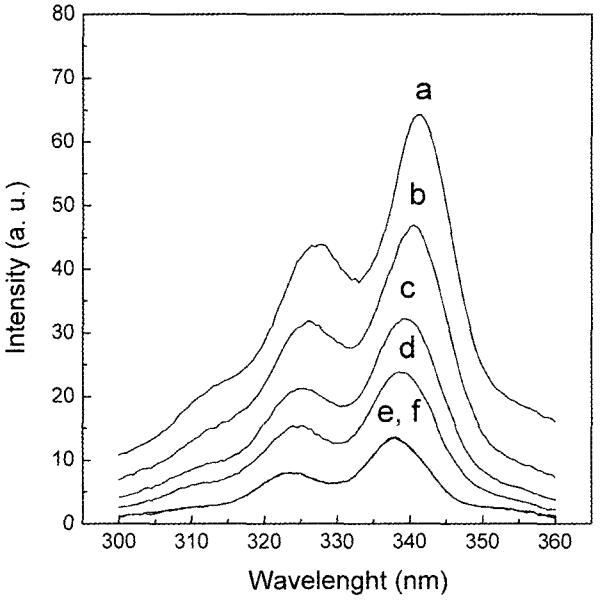

Figure 4. Excitation spectra of pyrene in PBS solution (pH=7.4) in the presence of DGC30; (a) 1, (b) 0.5 (c) 0.2, (d) 0.1, (e) 0.01, and (f) 0.001 mg/mL (adapted from Ref. [29]).

slightly increase with increasing DS in the case of each bile acid. In particular, the hydrophobicities of the inner cores mainly depend on the hydrophobicity of the bile acid. The K_v value of the CGC nanoparticles was 10 times higher than that of the DGC nanoparticles. The hydrophobicity of the nanoparticles may affect the loading efficiency of some substances and the stability of the nanoparticles in systemic circulation. The aggregation number per hydrophobic core (N_{bile}) and the number polymer chains per hydrophobic core (N_{chains}) are listed in Table II. Based on the cetylpyridinium chloride (CPC) quenching kinetics, the number of hydrophobic cores in each nanoparticle could be estimated from the slope of the plot of $\ln(I_{343}/I_{338})$ of the pyrene fluorescence

Table II. Microscopic Characteristics of Self-Aggregates Determined by Fluorescence Probe Method

Sample	cac[a]	K_v[b](10^{-4})	N_{bile}[c]	N_{chain}[d]
DGC 6	0.260	0.4	13	2.3
DGC 11	0.160	0.5	30	2.6
DGC 22	0.076	0.7	64	3.0
DGC 30	0.038	0.8	118	3.9
CGC1	0.219	2.4	109	8.6
CGC5	0.112	3.1	359	6.8
CGC12	0.047	4.0	814	5.5

[a]Critical aggregation concentration determined from the excitation spectra of pyrene. [b]Binding equilibrium constant of pyrene in the presence of DGCs and CGCs. [c]Aggregation number of bile acids per one hydrophobic domain. [d]The number of polymer chains per one hydrophobic domain.

as a function of the CPC concentration in the presence of the BGC nanoparticles.[29,31] The aggregation number per single hydrophobic core in the BGC nanoparticles, N_{bile}, was in the range of 13-814. These N_{bile} values were much higher than the aggregation number of free deoxycholic acid in aqueous media (8±2), because of the limited mobility and steric hindrance of the bile acids in the glycol chitosan chains.[33] It was also found that from 2.3 to 8.6 chains of BGC derivatives formed on the hydrophobic core, and that the value of N_{chain} did not vary with the hydrophobicity of the BGC nanoparticles, mainly because of the stiffness of the glycol chitosan chains. These microscopic characteristics of the BGC nanoparticles suggested that a small number of BGC chains (less than 9) could form one hydrophobic core, and that the BGC nanoparticles form the multicore structure in each nanoparticle, perhaps in a similar fashion to the multicore structure of biopolymers hydrophobically modified with various fatty acid and bile acids, as shown in Figure 5.[26,29]

Stability of BGC Nanoparticles in Physiological Conditions. Methods of delivery employing polymeric nanoparticles have taken center stage, because they allow drugs to be passively targeted to the tumor site by utilizing the EPR effect.[9,12] Therefore, the stability of polymeric nanoparticles in physiological conditions is very important for the successful delivery of the drugs to the target tumor tissues. It is known that the application of chitosan-based nanoparticles, which are biocompatible, biodegradable and have low toxicity, is limited by their low solubility in physiological conditions (pH=7.4, ionic strength=0.15).[25] Also, there is a possibility of inducing cytotoxicity owing to the use of acetic acid, since chitosan is dissolved in water containing acetic acid.[23,24] Thus, clinical trials using chitosan-based nanoparticles have not been able to be performed, because their insolubility in physiological conditions leads to their aggregation and precipitation within a few days.[19,20]

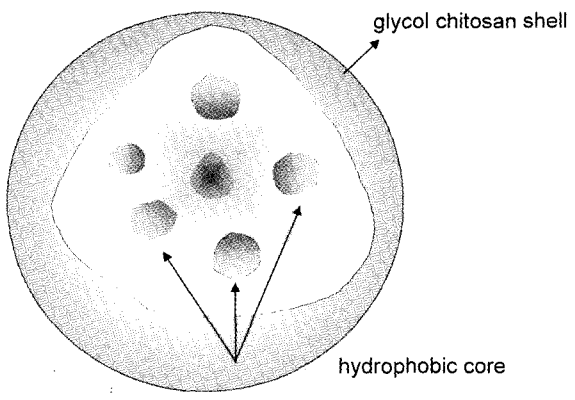

Figure 5. Schematic representation of the multicore structure of the BGC nanoparticles.

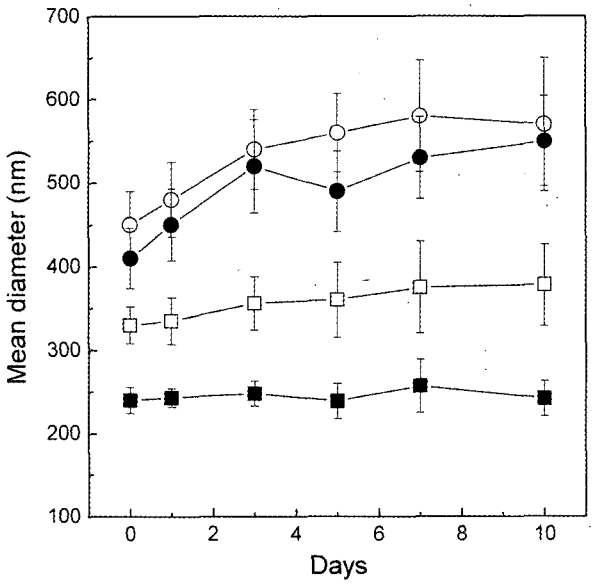

Figure 6. Time course of changes in mean size for DGC nanoparticles (1mg/mL) at 36 °C in PBS (pH = 7.4, ionic strength = 0.15) solution: (○) DGC6, (●) DGC11, (□) DGC22, (■) DGC30 (adapted from Ref. [29]).

The stability of the DGC nanoparticles in PBS solution (pH=7.4 ionic strength=0.15) at 37 °C was found to be mainly dependant on the DS of deoxycholic acid (Figure 6). The results indicated that the mean size of the DGC nanoparticles increased with increasing incubation time when the DS value of deoxycholic acid was lower than 12. However, the mean diameter of the DGC nanoparticles with a higher DS of deoxycholic acid did not vary with increasing incubation time, but showed a very narrow size distribution. Based on the microscopic characteristics of the self-aggregates, increasing the DS enhances the hydrophobicity of the inner cores, and this increase in hydrophobicity may counteract the aggregation of self-aggregates with a broad size distribution. Consequently, the DGC nanoparticles main-

tained their self-aggregate structure in physiological conditions and this stability was maintained for 10 days.

BGC Nanoparticles for Cancer Therapy

Biodistribution of BGC Nanoparticles. The usefulness of polymeric nanoparticles is limited by their massive capture by the RES in the liver and spleen after their intravenous administration. Hence, a drug delivery system is needed that avoids the RES and is be able to localize to the tumor tissues (Figure 7). Although the role of polymeric nanoparticles in cancer therapy has already been extensively studied, several problems remain to be overcome, such as their low drug entrapment efficiency, short retention time in the tumor site, biocompatibility, biodegradability, etc.[34-36]

The biodistribution of BGC nanoparticles was analyzed with FITC-labeled BGC nanoparticles having a mean diameter of 250 nm, because these fluorescently labeled nanoparticles provide a rapid, simple, and sensitive method of quantifying the biodistribution of nanoparticles by fluorometry. On the 7th day after the inoculation of tumor cells (II45 mesothelioma) in male Fisher 344 rats, BGC nanoparticles in 0.9% saline solution were injected into the tail vein of the tumor-bearing rats at a dose of 10 mg/kg. The blood and tissue distribution of the BGC nanoparticles at 1, 3 and 8 days after their i.v. injection in the tumor-bearing rats is shown in Figure 8. The BGC nanoparticles were distributed mainly in the kidneys, liver, and tumor tissues and were virtually absent from the other tissues. In particular, the BGC nanoparticles still circulated at a high level in the blood throughout the 8 day study period, implying their long systemic retention in the blood circulation. Very few BGC nanoparticles were observed in the tumor tissues until one day after injection. However, at 3 days after injection, the increase in the level of the BGC nanoparticles in the tumor tissues was significant. At 8 days after injection, the amount of BGC nanoparticles in the tumor tissues was remarkably increased. On the other hand, the amount of BGC nanoparticles in the liver gradually decreased over the 8 day period. From the biodistribution results, it was concluded that the BGC nanoparticles were retained for 8 days in the systemic circulation after their intravenous administration, and that their enhanced biodistribution allowed them to accumulate and extravagate into the tumor tissues due to the EPR effect.

RGD Peptide Loaded CGC Nanoparticles for Cancer Therapy. It has been known that angiogenesis is a representative hallmark of cancer.[37,38] Since endothelial cells in the angiogenic vessels express several markers, which are either barely detectable or entirely absent in normal blood vessels.[39-41] Of the makers expressed, $\alpha_v\beta_3$ integrin has much attention because its level of expression in the tumor vasculature correlates with the degree of malignancy and proliferation of tumor.[42,43] For the targeting $\alpha_v\beta_3$ integrin, several *in vivo* studies exhibited that antibodies, small inhibitory peptides bearing Arg-Gly-Asp (RGD) sequence, and antiagonists of $\alpha_v\beta_3$ integrins have thus been developed as potential antiangiogenic strategies.[44-46] These various antiangiogenic substances have also been used as imaging agents to detect angiogenesis in tumors. However, it should be noted that several of these antiangiogenic substances are susceptible to enzymatic degradation in the blood circulation,[47] and cannot substantially reach the target site via systemic administration, because of their rapid elimination by renal filtration and the RES system. Therefore, appropriate drug carriers that can surmount these different biological barriers are very much needed.

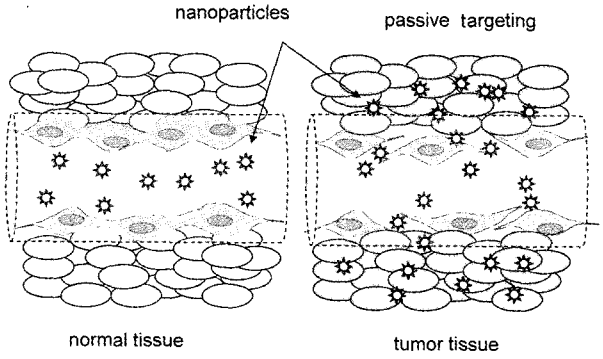

Figure 7. Schematic representation of the passive targeting associated with the EPR effect in tumor tissues.

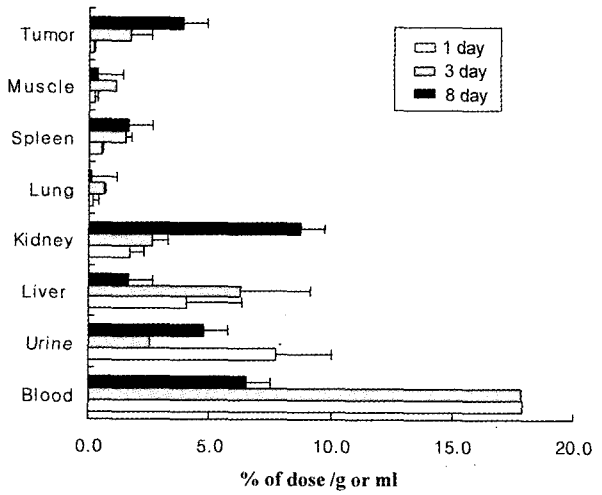

Figure 8. Tissue distribution of FITC-labeled BGC nanoparticles 1, 3 and 8 days after i.v. injection in tumor-bearing rats at a dose of 10 mg/kg. Each column represents the mean value (n=6). Data are represented as means ± S.D. (adapted from Ref. [27]).

To overcome these biological barriers, CGC nanoparticles (DS value; 12, diameter; 210 nm) were used as a carrier for the FITC-labeled RGD peptide (FITC-GRGDS) and FITC-labeled RAD peptide (FITC-GRADS) as a negative control. These two FITC-labeled peptides were encapsulated into CGC nanoparticles under three different conditions: simple

mixing, sonication, and the solvent evaporation method.[28] Of these different methods, solvent evaporation showed the most promising results for peptide loading, as judged by the yield (>70%) and loading efficiency (>75%). Figure 9 shows the release profiles of FITC-GRGDS and FITC-GRADS as a function of time. The FITC-labeled RGD peptides were released from the nanoparticles with the peptide content of 33.8 wt% in physiological solution (pH=7.4) for up to 1 day. Both of the FITC-labeled peptides exhibited similar release behavior: for the initial 6 h, 73% of the peptides loaded were released at an almost constant rate, followed by a slower release for the remaining duration of time. The water-soluble nature of both FITC-labeled peptides, which is ascribed to their hydrophilicity, might govern the release pattern, in conjunction with various aspects of their physical interaction with the CGC nanoparticles, such as their hydrophobic interaction, hydrogen bonding, and electrostatic interaction. To demonstrate that the FITC-GRGDS can act as a specific ligand for $\alpha_v\beta_3$ integrin, their binding and subcellular localization were studied by incubating them with HUVECs that are known to overexpress $\alpha_v\beta_3$ integrin.[48] As expected, FITC-GRGDS specifically bound to the HUVECs and also prevented their migration on the surface coated with $\alpha_v\beta_3$ integrin, indicating its specific binding to $\alpha_v\beta_3$ integrin. However, FITC-GRADS did not affect the adhesion and migration of the HUVECs. The detailed effect of RGD peptide-loaded CGC nanoparticles, in terms of their ability to image or destroy the angiogenic vessels surrounding the tumor tissues, is currently under investigation *in vivo*.

The Use of Doxorubicin Loaded Glycol-Chitosan Nanoparticles for Cancer Therapy. One of the most potent and widely used anticancer drugs is doxorubicin, which prevents the synthesis of nucleic acids within cancer cells.[49] However, doxorubicin has a number of undesirable side effects such as cardiotoxicity and myelosuppression, which lead to its having a very narrow therapeutic index. Thus, extensive studies have been conducted utilizing doxorubicin coupled or encapsulated to various polymeric nanoparticles, in an attempt to minimize the undesirable side effects of free doxorubicin by using the EPR effect.[50, 51]

For the *in vivo* tumor targeting of doxorubicin, glycol chitosan-doxorubicin conjugates (GC-DOX) were synthesized using EDC chemistry.[28] *N-cis*-aconityl doxorubicin was directly coupled to glycol chitosan using EDC and NHS, because the *cis*-aconityl spacer in doxorubicin is hydrolyzed in acidic conditions and, consequently, free doxorubicin can be freely released from the nanoparticles after its hydrolysis in the tumor site.[52] The synthesized GC-DOX with a doxorubicin content in the range of 2.0 and 5.0 wt% formed stable nanoparticles in aqueous media, but the GC-DOX with a doxorubicin content of more than 5.5 wt% was precipitated in aqueous media, due to its excessive hydrophobicity. The morphology of the GC-DOX nanoparticles was observed by TEM (Figure 10). The nanoparticles had a nearly spherical shape with a diameter ranging from 100 to 200 nm and their size distribution was fairly uniform.

Free doxorubicin was also physically encapsulated into GC-DOX nanoparticles by the o/w emulsion method. A loading content of doxorubicin into the GC-DOX nanoparticles as high as 38 wt% was obtained, along with a loading efficiency of 97%. After the encapsulation of doxorubicin, the size of the GC-DOX nanoparticles increased slightly to 300 nm. The *in vitro* release of doxorubicin from the GC-DOX nanoparticles in different pH media is shown in Figure 11. Under *in vitro* conditions, doxorubicin was released more slowly at pH 7 than at pH 4. This indicates that, at higher pH, glycol chitosan retains its hydrophobicity and that the hydrolysis of the doxorubicins coupled to the glycol

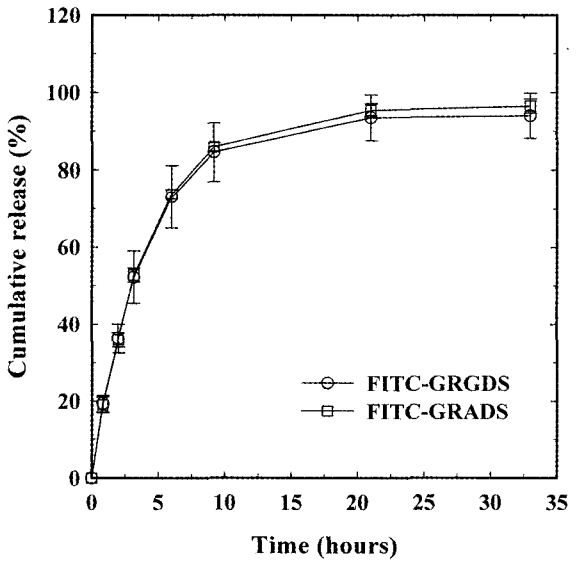

Figure 9. Release profiles of FITC-labeled peptides from CGC nanoparticles with the peptide content of 33.8% were exposed to at 37 °C in PBS buffer (pH=7.4). The error bar represents standard deviation (n=5) (adapted from Ref. [28]).

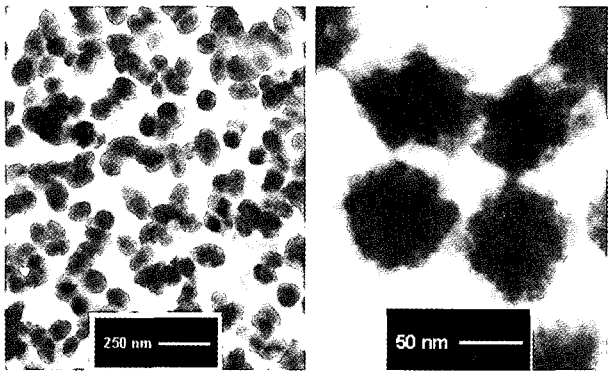

Figure 10. Transmission electron microscopy (TEM) images of doxorubicin-conjugated glycol chitosan (GC-DOX) nanoparticles (adapted from Ref. [27]).

chitosan chains is also prevented.

The *in vivo* anti-tumor activities of free doxorubicin and the GC-DOX nanoparticles were studied using male Fisher 344 rats. The intravenous route through the tail vein was selected for the injection of the free DOX or GC-DOX nanoparticles physically loaded with 38 wt% free doxorubicin into the tumor-bearing rats (II45 mesothelioma). The size of the tumor was significantly suppressed ten days after the i.v. injection of the GC-DOX nanoparticles (Figure 12). In addition, the body weight of the GC-DOX nanoparticle treated rats remained constant, while that of the free doxorubicin treated rats significantly decreased over the 10 day period (Figure 13). This indicates that free doxorubicin was distributed not only in the tumor cells, but also in other normal cells that might suffer from various side effects. However, the GC-DOX nanoparticles were mainly accumulated in the tumor site.

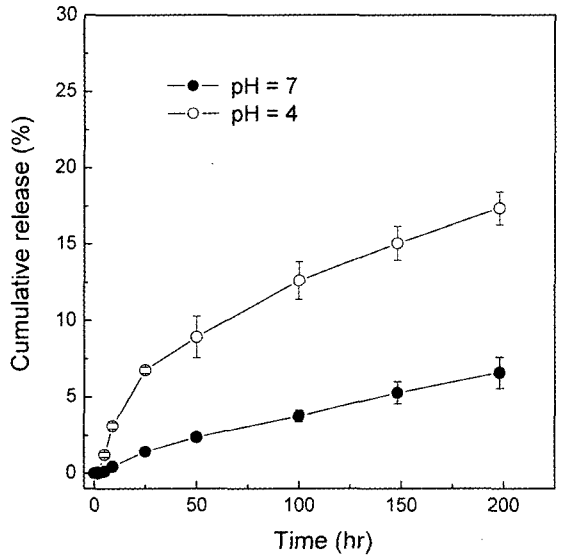

Figure 11. Effect of pH on the release profile of doxorubicin loaded GC-DOX nanoparticles. Release profile measured by fluorometer. Each point is the mean of three replicates. Data are represented as means ± S.D. (adapted from Ref. [27]).

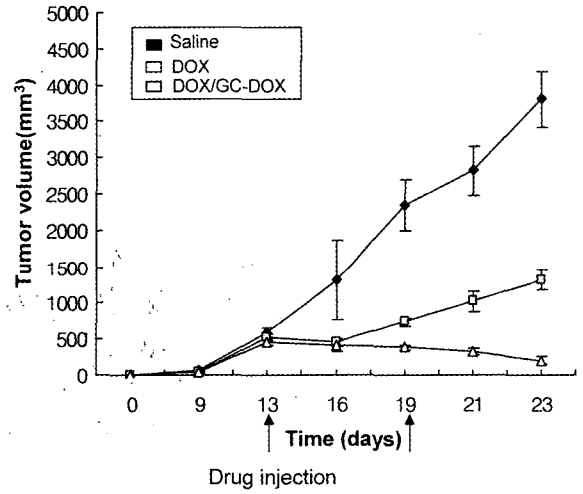

Figure 12. *in vivo* anti-tumor activity of free doxorubicin and doxorubicin loaded GC-DOX nanoparticles after i.v. injection in the back of tumor-bearing rats at a dose of 10 mg/kg. Each column represents the mean value (n=6). Data are represented as means ± S.D. (adapted from Ref. [27]).

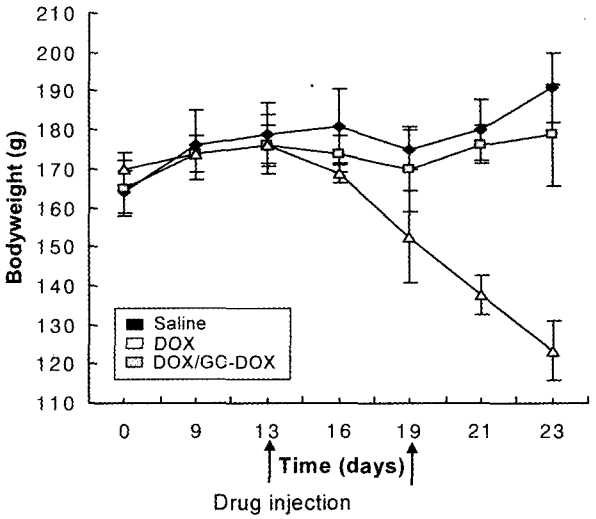

Figure 13. Body weight distribution of free doxorubicin group, doxorubicin loaded GC-DOX nanoparticles treated group and control after i.v. injection in the back of tumor-bearing rats at a dose of 10 mg/kg. Each column represents the mean value (n=6). Data are represented as means ± S.D. (adapted from Ref. [27]).

Conclusions

Glycol chitosan, a water soluble chitosan derivative, is one of the most biocompatible and biodegradable polysaccharides. Bile acid-modified glycol chitosan derivatives and anticancer drug modified glycol chitosan derivatives can be readily prepared using EDC chemistry. The physicochemical properties, such as nanoparticle size, hydrophobicity, and biostability of the various BGC nanoparticles, could be achieved by grafting different amounts of bile acids. These hydrophobically modified glycol chitosan derivatives formed a uniform nanoparticle structure in physiological conditions. Glycol chitosan-based nanoparticles can function well as a drug carrier, due to their long systemic retention, low toxicity and accumulation in the tumor tissues. Further, more *in vivo* studies need to be carried out to optimize this potential drug carrier for cancer therapy.

Acknowledgements. This study was supported by the Real Time Molecular Imaging Project of the KIST Intramural Research Program, Korea and the Regional Technology Innovation Program of the Ministry of Commerce, Industry

and Energy (MOCIE) (grant No. RTI04-01-01).

References

(1) K. Akiyoshi and J. Sunamoto, *Surfactants Sci. Ser.*, **44**, 289 (1992).
(2) K. Akiyoshi, S. Deguchi, N. Moriguchi, S. Yamaguchi, and J. Sunamoto, *Macromolecules*, **26**, 3062 (1993).
(3) R. Gref, Y. Minamitake, M. T. Peracchia, V. Trubetskoy, V. Torchilin, and R. Langer, *Science*, **263**, 1600 (1994).
(4) Y. Nagasaki, K. Yasugi, Y. Yamamoto, A. Harada, and K. Kataoka, *Biomacromolecules*, **2**, 1067 (2001).
(5) K. Kataoka, A. Harada, and Y. Nagasaki, *Adv. Drug. Deliv. Rev.*, **47**, 113 (2001).
(6) G. S. Kwon and T. Okano, *Adv. Drg Deliv. Rev.*, **21**, 107 (1996).
(7) H. S. Yoo and T. G. Park, *J. Control. Release*, **70**, 63 (2001).
(8) Y. Matsumura and H. Maeda, *Cancer Res.*, **46**, 6387, (1986).
(9) Y. Matsumura and H. Maeda, *Cancer Res.*, **46**, 6387, (1986).
(10) G. S. Kwon, M. Naito, M. Yokoyama, T. Okano, Y. Sakurai, and K. Kataoka, *Pharm. Res.*, **12**, 192 (1995).
(11) M. Yokoyama, S. Inoue, K. Kataoka, N. Yui, T. Okano, and Y. Sakurai, *Macromol. Chem.*, **190**, 2041, (1989).
(12) M. Yokoyama, M. Miyauchi, N. Yamada, T. Okano, Y. Sakurai, K. Kataoka, and S. Inoue, *Cancer Res.*, **50**, 1693, (1990)
(13) H. Hashizume, P. Baluk, S. Morikawa, J. McLean, G. Thurston, S. Roberge, R. K. Jain, and D. M. McDonald, *Am. J. Pathol.*, **156**, 1363, (2000).
(14) Q. Li, E. T. Lunn, E. W. Grandmaison, and M. F. A. Goosen, in *Applications of Chitin and Chitosan*, M. F. A. Goosen, Ed., Technomic Publishing Co., Inc., Lancaster, 1997, p. 3.
(15) E. Ruel-Gariepy, G. Leclair, P. Hildgen, A. Gupta, and J. C. Leroux, *J. Control. Release*, **82**, 373 (2002).
(16) Y. Zhang and M. Zhang, *J. Biomed. Mater. Res.*, **62**, 378, (2002).
(17) I. F. Uchegbu, L. Sadiq, M. Arastoo, A. I. Gray, W. Wang, R. D. Waigh, and A. G. Schätzleinä, *Int. J. Pharm.*, **224**, 185 (2001).
(18) X. G. Chen, C. M. Lee, and H. J. Park, *J. Agric. Food Chem.*, **51**, 3135 (2003).
(19) K. Y. Lee, W. H. Jo, I. C. Kwon, Y. Kim, and S. Y. Jeong, *Macromolecules*, **31**, 378 (1998).
(20) K. Y. Lee, I. C. Kwon, Y. H. Kim, W. H. Jo, and S. Y. Jeong,, *J. Control. Release*, **51**, 213 (1998).
(21) Y. H. Kim, S. H. Gihm, C. R. Park, K. Y. Lee, T. W. Kim, I. C. Kwon, H. Chung, and S. Y. Jeong, *Bioconjugate Chem.*, **12**, 932 (2001).
(22) C. Qin, Y. Du, L. Xiao, Z. Li, and X. Gao, *Int. J. Bio. Macromol.*, **69**, 97 (2002).
(23) M. Yalpani and L. D. Hall, *Macromolecules*, **17**, 272 (1984).
(24) M. Sugimoto, M. Morimoto, H. Sashiwa, H. Saimoto, and Y. Shigemasa, *Carbohydr. Polym.*, **36**, 49 (1998).
(25) T. H. Kim, I. K. Park, J. W. Nah, Y. J. Choi, and C. S. Cho, *Biomaterials*, **25**, 3783 (2004).
(26) S. Kwon, J. H. Park, H. Chung, I. C. Kwon, S. Y. Jeong, and I. Kim, *Langmuir*, **19**, 10188 (2003).
(27) Y. J. Son, J. S. Jang, Y. W. Cho, H. Chung, R.W. Park, I. C. Kwon, I. Kim, J. Y. Park, S. B. Seo, C. R. Park, and S. Y. Jeong, *J. Control. Release*, **91**, 135 (2003).
(28) J. H. Park, S. Kwon, J. Nam, R. Park, H. Chung, S. B. Seo, I. Kim, and I. C. Kwon, *J. Control. Release*, **95**, 579 (2004).
(29) K. Kim, S. Kwon, J. H. Park, H. Chung, S. Y. Jeong, and I. C. Kwon, *Biomacromolecules*, **6**, 1154 (2005).
(30) A. Enhsen, W. Kramer, and Wess, *Drug Discov. Today*, **3**, 409 (1998).
(31) M. Wilhelm, C. Zhao, Y. Wang, R. Xu, M. A. Winnik, J. Mura, G. Riess, and M. D. Croucher, *Macromolecules*, **24**, 1033 (1991).
(32) K. M. Huh, S. C. Lee, S. W. Kang, I. C. Kwon, Y. Kim, and S. Y. Jeong, *Langmuir*, **16**, 10566 (2000).
(33) S. Barnes, and D. N. Kirk, in *The Bile Acids, chemistry, Physiology, and Metabolism*, K. K. R. Setchell, D. Kritchevsky, and P. P. Nair, Eds., Plenum Press, New York, 1988, vol. 4, p. 68.
(34) G. D. Grossfeld, R. R. Carrol, and N. Lindeman, *Urology*, **59**, 97 (2002).
(35) H. Hashizume, P. Baluk, S. Morikawa, J. McLean, G. Thurston, S. Roberge, R.K. Jain, and D.M. McDonald, *Am. J. Pathol.*, **156**, 1363 (2000).
(36) S. K. Hobbs, W. L. Monsky, F. Yuan, W. G. Roberts, L. Driffith, V. P. Torchilin, and R. K. Jain, *Med. Sci.*, **95**, 4607 (1998).
(37) P. Carmeliet and R. K. Jain, *Nature*, **407**, 249 (2000).
(38) E. Ruoslahti, *Nat. Rev. Cancer*, **2**, 83 (2002).
(39) M. Friedlander, P. C. Brooks, R. W. Shaffer, C. M. Kincaid, J. A. Varner, and D. A. Cheresh, *Science*, **270**, 1500 (1995).
(40) H. P. Hammes, M. Brwonlee, A. Jonczyk, A. Sutter, and K. T. Preissner, *Nat. Med.*, **2**, 529 (1996).
(41) M. A. Burg, R. Pasqualini, W. Arap, E. Rouslahti, and W. B. Stallcup, *Cancer Res.*, **59**, 2869 (1999).
(42) P. C. Brooks, R. A. Clark, and D. A. Cheresh, *Science*, **264**, 569 (1994).
(43) A. Erdreich-Epstein, H. Shimada, S. Groshen, M. Liu, L. S. Metelitsa, K. S. Kim, M. F. Stins, R. C. Seeger, and D. L. Durden, *Cancer Res.*, **60**, 712 (2000).
(44) P. C. Brooks, A. M. Montgornery, M. Rosenfeld, R. A. Reisfeld, T. Hu, G. Klier, and D. A. Cheresh, *Cell*, **79**, 1157 (1994).
(45) B. P. Eliceiri and D. A. Cheresh, *J. Clin. Invest.*, **103**, 1227 (1999).
(46) H. N. Lode, T. Moehler, R. Xiang, A. Jonczyk, S. D. Gillies, D. A. Cheresh, and R. A. Reisfeld, *Proc. Natl. Acad. Sci. U. S. A.*, **96**, 1591 (1999).
(47) K. Park and R. J. Mrsny, *ACS Symposium Series*, American Chemical Society, Washington, DC, 2000, vol. 752, pp 2-12.
(48) J. O. Nam, J. E. Kim, H. W. Jeong, J. O. Nam, B. H. Lee, J. Y. Choi, R. W. Park, J. Y. Park, and I. S. Kim, *J. Bio. Chem.*, **278**, 25902 (2003).
(49) H. S. Yoo and T. G. Park, *Polymer Preparation*, **41**, 992 (2000).
(50) V. Omelyaneko, P. Kopečková, C. Gentry, and J. Kopeček, *J. Control. Release*, **53**, 25 (1998).
(51) M. Dvořák, P. Kopečková, and J. Kopeček, *J. Control. Release*, **60**, 321 (1999).
(52) Z. Zhu, J. Kralovec, T. Ghose, and M. Mammen, *Cancer Immunol. Immunother.*, **40**, 257 (1995).